Journal of Engineering and Applied Sciences 2 (3): 637-647, 2007

Non-Equilibrium Electron-Lattice Heating and Enhanced Free Carrier Concentrations in Nanosecond CO_2 Laser Pumped Semi-Conducting GaAs Thin Film

[1]D.K. De and [2]E.F. Musongong
[1]Department of Physics, Federal University of Technology, Yola Adamawa State, Nigeria
[2]Department of Physics, Nasarawa State University, Keffi Nigeria

Abstract: In this study, we have theoretically investigated the non-equilibrium electron-lattice heating in intrinsic Gallium-Arsenide thin film for various thicknesses, irradiated by few nanoseconds pulsed Carbon dioxide (CO_2) laser for various intensities incident normally on a thin film. It is shown by our numerical simulations that there is significant difference between the average transient hot electron temperature $\langle T_e(t)\rangle$ and the average lattice temperature $\langle T_l(t)\rangle$ of ~3000 K for a time scale considerably greater than the duration of the laser pulse, which gives rise to significantly enhanced free carrier concentration in the conduction band of the semiconductor. The possibility of enhanced photoemission of transient hot electron bunches from such laser pumped semi-conducting thin film by using a suitable delayed probe laser is discussed and proposed experimental set up.

Key words: Carrier concentration, average transient hot electrons, thickness of film, different intensities, specific heat and gallium-arsenide thin films

I INTRODUCTION

Fujimoto *et al.* (1984) studied theoretically and experimentally non-equilibrium electron Temperature (T_e) and lattice Temperature (T_l) in a polycrystalline tungsten sample irradiated (with normal incidence) by 75 femtosecond laser pluses of energy 0.4 mJ per pulse. They obtained experimentally enhanced photoemission (corresponding to 1000 A cm^{-2}) collected by a delayed probe pulse and determined an electron-phonon (e-ph) relaxation time (τ_{ep}) of the order of several hundred femtoseconds. It may be mentioned that the non-equilibrium electron relaxes to the lattice temperature through e-ph relaxation mechanism (Elseyed *et al.*, 1987; Kaganov *et al.*, 1956; Anisimov *et al.*, 1974; Fann *et al.*, 1992; Sun *et al.*, 1994; Wang *et al.*, 1994; Hertel *et al.*, 1996; Scheonlein *et al.*, 1988; Bechtel *et al.*, 1975; Yen *et al.*, 1980). However, when pulses are shorter than the electron-phonon relaxation time a decoupling between the electrons and the lattice temperatures can take place, generating the so-called anomalous heating effect (Damascelli *et al.*, 1996). The enhanced photoemission results through multiphoton nonlinear processes when there is considerable non-equilibrium temperature (in excess of ≈ 2000 K) of electrons in comparison to the lattice (Fuijimoto *et al.*, 1984; James, 1983).

The photo emitted current density of approximately 1000 Acm^{-2} indicates a total pulsed charge of approximately 75×10^{-12} Coulomb (75 pc) per pulse. For Free-electron laser of very high brightness and low emittance (Stephen, 2003; Wang, 2002), it would be highly desirable to obtain pulse photoemitted electron bunch of a few hundred nano Coulomb to one micro Coulomb charge. The above technique of pump probe enhanced photoemission cannot be extended to achieve this objective with femtosecond laser pulse, since the required pulse power would be far above the damage threshold of any metallic photocathode surfaces (Jensen *et al.*, 2003; Elsayed *et al.*, 1991). It may appear that pico Coulomb charge photo emitted electron pulse could have been obtained if picosecond laser pulses could have been used, instead of femtosecond pulses. However, the requirement for enhanced non-equilibrium temperature (say 3000 K) and thus enhanced photoemission is that, the time width of the high power laser pulse (however below the damage threshold as reported by Wu *et al.* (2001) laser pulse of energy 0.5 nJ did not impose obvious destruction on thin film) be shorter than electron-phonon relaxation time. It is hard to obtain such electron temperatures with picosecond laser pulse in metals, because the electron-phonon (e-ph) relaxation time is much shorter than the picosecond τ_{ep}. However, the

Corresponding Author: D.K. De, Department of Physics, Federal University of Technology, Yola Adamawa State, Nigeria

actual criterion for thermally enhanced photoemission electron-bunch of nano to micro-Coulomb charge is that there should be sufficient free electron concentration in the conduction band belonging to the high energy side of the Fermi distribution for sufficiently long time, so that these electrons can be photo emitted by a delayed nanosecond pulses. The electron-phonon coupling factor (Fujimoto *et al*., 1984).

$$\alpha = \frac{\pi^2 m n_e V_s^2}{6\tau_{ep} T_l} \quad (1)$$

(where m is the effective mass of the electron, n_e is the concentration of charge carrier and V is the velocity of sound) should be quite low so that the transient electron temperature T_e is very much greater than the lattice temperature T_l. It may be mentioned that α also changes dynamically during the laser irradiation which had not been taken in to account during the theoretical computation by Fujimoto, who used a constant α. The τ_{ep} in α should actually be related to the ordinary Drude model electron relaxation, τ_e, for electrical conductivity in metal or semiconductor, which for tungsten is ~10^{-14}s at 300 K.

It appears that τ_e is longer in semiconductors like intrinsic GaAs than in metals like W, Cu etc. The free electron concentration in semi conductors can be raised from very low values (…n_i= 9×10^6/cm^3 for intrinsic GaAs (Grove, 1967) to quite high values say 10^{19}/cm^3 and above by doping. This gives a way of controlling α in semiconductors, which could be made much lower than in metals. Moreover the electronic specific heat C_e (per unit volume) is expected to be much lower in semiconductors than in a metal, because of the lower Fermi energy E_F. Thus, it is quite likely that significant non-equilibrium electron-lattice temperature differences can be possible in suitable semi-conducting thin films with picosecond to nanosecond laser pulse irradiation.

MATERIALS AND METHODS

The above idea motivated us to investigate theoretically the non-equilibrium electron heating in semi-conducting thin films. We report here the non-equilibrium electron temperature calculated for intrinsic GaAs thin films of various thickness irradiated by few nanoseconds pulsed CO_2 laser of various intensities, assumed to be incident normally (along the z-direction) on the thin films. (Fig. 1). James (1983) has shown that CO_2 laser, though well below the band gap of GaAs and many other semi-conducting materials, can be absorbed by the semi-

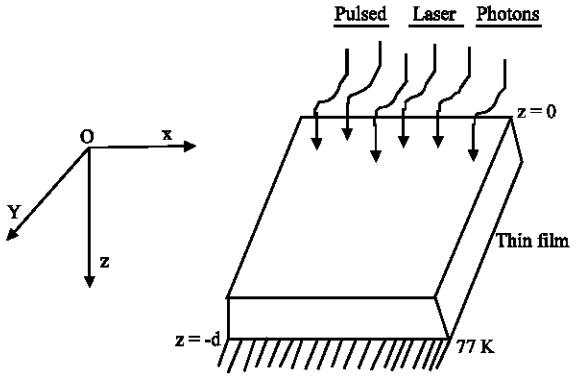

Fig. 1: Laser pulses incident normally on a thin film

conducting materials. The absorption process involves laser heating of the free electron distribution (in n-type semiconductors) to a point where significant fraction of the electron density have an energy greater than the band gap (as measured from the band gap minima). These highly energetic carriers can relax by creating electron-hole pairs through impact ionization process (inverse Auger event). This impact ionization processes can lead to the formation of a laser-induced plasma and with consequent increase in electron temperature and free carrier concentration. For a given laser pulse power intensity and duration, the net increase in electron temperature T_e and free electron concentration n_e, should depend on the thickness and properties of the semi-conducting materials, that are irradiated by the given laser pulse.

In this study, we studied these two dynamic processes (i.e., changing T_e and n_e) by treating the absorption of pulsed CO_2 laser through a process similar to that of femtosecod laser irradiation in tungsten (Fujimoto *et al*., 1984), however by considering the dynamic variation of T_e, n_e and C_e during the laser absorption.

Most of the non-equilibrium electron temperatures that have been calculated so far (only in metals) are those of surface electrons (Fujimoto *et al*., 1984; Jensen *et al*., 2003). For effective enhancement of photoemission, the realistic picture of electron temperature should be obtained by calculating the z-average of the electron temperature $T_e(z,t)$ over the thickness of the thin film. We call this average $\langle T_e(t)\rangle$. Thus

$$\langle T_e(t)\rangle = \lim_{\Delta z \to 0} \langle T_e(z,t)\rangle_z$$

defines the temperature that would be expected if all the electrons in different layers z_i, with different $T_e(z_i,t)$ values

thermalize at the instant of time t. If the back of the film is maintained at 77K, the electron mean free path can be longer than that at room temperature (since the lattice temperature is virtually unaffected) and the electron can escape from a greater depth than at room temperature, contributing to the enhancement.

For the effective enhancement of the pulsed photoemitted electron bunch, the $\langle T_e(t)\rangle$ needs to be sufficiently high without causing any material damage. The maximum total electron concentration (bound and free) in an intrinsic GaAs sample

$$N = \frac{4\rho \times 6.03 \times 10^{23}}{9} cm^{-3},$$

Where ρ is the density of the material (ρ = 5.32 g cm^{-3}). To have a safety factor of 10 in order not to have material damage (which can take place when all the bound electrons are excited to the conduction band, leading to transient hot free electron concentration n_e approaching to that of N) we should not allow n_e to exceed 1.4×10^{23} cm^{-3} as a result of laser pumping. As a first approximation we have estimated n_e in GaAs sample for different T_e as shown in the (Table 1-4) using Eq. 2.

$$n_e = \left\{2\left(2\pi K_B T_e/\hbar_2\right)^{3/2}\left(M_e^* M_h^*\right)^{3/4}\exp\left(-E_g/2K_B T_e\right)\right\} \quad (2)$$

where E_g is the energy gap, M_e^*; M_h^* are the effective mass of electron and hole, respectively. Here we used $M_e^* = M_h^* = 0.07M_e$ and E_g = 1.43 eV (Lin and Chen, 1981). The required thickness d_l of the semi-conducting thin film for a given pulsed CO_2 laser intensity and duration of laser pulses etc. can be determined (for the practical photoemission experiment) based on the following computations keeping the above safety figure in view. When α is low, the lattice heating is insignificant in comparison to the electron heating. In our calculation of $\langle T_e(t)\rangle$, we assume the band gap of the semiconductor to remain unchanged. This assumption is justified as long as the laser intensity is below the damage threshold and since the lattice heating is insignificant. Thus we allow n_e to vary dynamically during the laser heating and hence α and other parameters such as C_e etc (see below). The τ_{ep} is also dependent on T_e. We allowed τ_{ep} varying with T_l according to the following equation

$$\frac{1}{\tau_{ep}} = aT_l + bT_l^3 \quad (3)$$

where a and b are constants

Table 1: First approximation $T_e(t)$ K, $t\times10^{-10}$(s), $N_e(t)$ m^{-3}

$T_e(t)$ K	$t\times10^{-10}$(s)	$N_e(t)$ m^{-3}
300	-	4.5225×10^{11}
400	-	7.0075×10^{14}
600	1.75	1.2956×10^{18}
800	3.75	6.3282×10^{19}
1000	4.25	7.0384×10^{20}
1200	5.25	3.6881×10^{21}
1400	6.00	1.2479×10^{22}
1600	7.00	3.1983×10^{22}
1800	7.75	6.7900×10^{22}
2000	8.50	1.2609×10^{23}
2200	9.75	2.1211×10^{23}
2300	11.00	2.6714×10^{23}
2200	12.75	2.1211×10^{23}
2000	14.00	1.2609×10^{23}
1800	15.25	6.7900×10^{22}
1600	16.00	3.1983×10^{22}
1400	16.75	1.2479×10^{22}
1200	17.50	3.6881×10^{21}
1000	18.25	7.0384×10^{20}
800	19.00	6.3282×10^{19}
600	20.00	1.2956×10^{18}
400	22.25	7.0075×10^{14}
300	25.75	4.5225×10^{11}

Transient electron temperature profile enhanced free electron concentration in intrinsic GaAs with $\tau = 10^{-9}$ seconds. A_0 = 5 MW cm^{-2}, d = 280A^0

Table 2: GaAs sample $T_e(t)$ K, $t\times10^{-10}$(s), $N_e(t)$ m^{-3}

$T_e(t)$ K	$t\times10^{-10}$(s)	$N_e(t)$ m^{-3}
400	-	7.0075×10^{14}
600	1.00	1.2956×10^{18}
800	2.00	6.3282×10^{19}
1000	3.00	7.0384×10^{20}
1200	3.75	3.6881x 10^{21}
1400	4.25	1.2479×10^{22}
1600	4.50	3.1983×10^{22}
1800	5.00	6.7900×10^{22}
2000	5.50	1.2609×10^{23}
2200	6.00	2.1211×10^{23}
2400	6.75	3.3093×10^{23}
2600	7.00	4.8682×10^{23}
2800	7.75	6.8336×10^{23}
3000	8.25	9.2340×10^{23}
3100	9.75	1.0605×10^{24}
3000	11.25	9.2340×10^{23}
2800	12.25	6.8336×10^{23}
2600	13.00	4.8682×10^{23}
2400	13.50	3.3093×10^{23}
2200	14.00	2.1211×10^{23}
2000	14.50	1.2609×10^{23}
1800	15.00	6.7900×10^{22}
1600	15.50	3.1983×10^{22}
1400	16.00	1.2479×10^{22}
1200	16.50	3.6881×10^{21}
1000	17.50	7.0384×10^{20}
800	17.75	6.3282×10^{19}
600	18.75	1.2956×10^{18}
400	20.50	7.0075×10^{14}

Transient electron temperature profile enhanced free electron concentration in intrinsic GaAs with $\tau = 10^{-9}$ seconds. A_0 = 50 MW cm^{-2}, d = 100A^0

In semiconductor, the electronic specific heat C_e at a temperature ideally be given by

$$C_e = \frac{dE_T}{dT_e}, \quad \text{where} \quad E_T = \int_{Ec}^{\infty} E\, f(E)g(E)dE \quad (4)$$

Table 3: M^*_e; M^*_h are the effective mass of electron and hole

T_e(t) K	t×10^{-10}(s)	N_e(t) m^{-3}
300	-	4.5225×10^{11}
400	2.00	7.0075×10^{14}
500	3.75	6.2067×10^{16}
600	5.00	1.2956×10^{18}
700	6.50	6.2067×10^{18}
800	7.75	6.3282×10^{19}
860	9.75	1.4542×10^{20}
800	12.00	6.3282×10^{19}
700	13.00	6.2067×10^{18}
600	14.75	1.2956×10^{18}
500	15.75	6.2067×10^{16}
400	17.50	7.0075×10^{14}
300	23.25	4.5225×10^{11}

Transient electron temperature profile enhanced free electron concentration in intrinsic GaAs with $\tau = 10^{-9}$ seconds. $A_0 = 50$ MW cm^{-2}, $d = 1000A^0$

Table 4: Different absorbed power A = 1.4MW cm^{-2}

T_e(t)K	t×10^{-10}(s)	N_e(t) m^{-3}
400	2.00	7.0075×10^{14}
500	3.75	6.2067×10^{16}
600	5.00	1.2956×10^{18}
700	6.50	6.2067×10^{18}
800	7.50	6.3282×10^{19}
850	9.75	1.2764×10^{20}
800	12.25	6.3282×10^{19}
700	13.50	6.2067×10^{18}
600	14.50	1.2956×10^{18}
500	16.00	6.2067×10^{16}
400	17.75	7.0075×10^{14}
300	24.50	4.5225×10^{11}

Transient electron temperature profile enhanced free electron concentration in intrinsic GaAs with $\tau = 10^{-9}$ seconds. $A_0 = 15$ MW cm^{-2}, $d = 1000A^0$,

where

$$f(E) = \frac{1}{1+e^{(E-E_f)/K_BT_e}}$$

and g(E) is the density of the energy state given by

$$g(E) = \frac{M_e^*}{\hbar^2\pi^2}\sqrt{\frac{2M_e^*(E-E_c)}{\hbar^2}} = A'\sqrt{(E-E_c)}$$

where

$$A' = \frac{M_e^*\sqrt{2M_e^*}}{\hbar^3\pi^2} \text{ and } M_e^*$$

is given in (2). In semiconductors usually $E_f < E_c$ and with the laser heating, $E >> E_f < E_c$,

$$C_e(T_e) = \frac{d}{dT_e}\int_{Ec}^{\infty} Ee^{-\frac{(E-E_f)}{K_BT_e}} g(E)dE$$
$$= \frac{A}{K_BT_e^2}e^{-Eg/K_BT_e}\left[\beta^{7/2}\sqrt{7/2} + E_g\beta^{5/2}\sqrt{5/2}\right] \quad (5)$$

where $\beta = K_BT_e$ and

$$A = \left(2\pi K_B/\hbar^2\right)^{\frac{3}{2}}\left(M_e^*M_h^*\right)^{\frac{3}{4}}$$

is defined in (2).

We assume that the incident laser pulse has uniform energy density in the x-y plane and varies as $e^{-\mu z}$ for z>0 (Fig. 1), where μ is the absorption coefficient (Lin and Cheng, 1981). Thus

$$I(z,t) = I(t)e^{-\mu z} \quad (6)$$

For transient electrons heating, for z > 0 we take

$$\frac{C_e\partial T_e}{\partial t} = K_t\frac{\partial^2 T_e}{\partial z^2} - \alpha(T_e - T_l) + I'(z,t) \quad (7)$$

I' (z,t) is the gradient of the laser intensity I(z,t) at a depth z below the surface at z = 0 (Fig. 1) and K_t thermal conductivity (K_t = 0.81 W/cm^0K).

In our present case, we assume that most of the incident laser energy (apart from that reflected out) is absorbed first by the conduction band electron at z = 0 in the thin film. These electrons through electronic thermal conductivity, rapidly transfer the energy to electrons below z = 0 (i.e., z>0). The lattice receives energy from the electrons through electron-phonon coupling factor as in the equation

$$C_l\frac{\partial T_l}{\partial t} = \alpha(T_e - T_l) \quad (8)$$

and C_l for T_l>300K is assumed to follow Dulong-Petit's law.

The impact ionization process during the absorption of pulsed CO_2 laser power by the semi-conducting thin film also leads to growth of carriers by pumping the electrons from valence band to conduction band. Increased electrons in the conduction band with T_e Eq. 2 as laser power is absorbed, leads to increase of both C_e through Eq. 5. This will in turn lead to slowing down the rate of rise of T_e in time during laser irradiation from that of the initial switching on. In this calculations unlike that of Bloembergen and Jensen, we have allowed the electron-photon coupling α to be dynamic for GaAs thin film i.e., as the pump laser energy is absorbed by electrons in conduction band, α also changes according to Eq. 1 due to the dynamic nature of n_e. However, we assumed the sound velocity V_s to be constant (V_s = 5.22×10^3 cm/sec), since the lattice heating is insignificant (as can be seen latter).

For a thin semi-conducting film with pump laser incident along the z-direction, the transient electron heating is at z = 0 governed by the following conditions with I(t) assumed to have the following forms

$$I(t) = I_0(1-R)\exp\left(-\left\{\frac{t-\tau}{2\tau}\right\}^2\right) \text{ for Gaussian pluse} \quad (9a)$$

$$I(t) = I_0(1\text{-}R) \text{ for } 0 \le t \le \tau,\ I(t) = 0, \text{ for } t \ge \tau \text{ for square pulse} \quad (9b)$$

where R is surface reflectivity. In our present calculations we have ignored any thermal radiations from the thin films owing to hot electrons.

The absorption of power from the incident laser pulse at z = 0 is

$$\frac{dU}{dt} = \left(\frac{C_e \partial T_e}{\partial t}\right)_{z=0} + \left(\frac{C_l \partial T_l}{\partial t}\right)_{z=0}$$

$$\text{and this equal to} -\left(\frac{dI}{dz}\right)_{z=0}. \text{ Thus} \quad (10)$$

$$\left(\frac{C_e \partial T_e}{\partial t}\right)_{z=0} + \left(\frac{C_l \partial T_l}{\partial t}\right)_{z=0} = \left(\frac{dI}{dz}\right)_{z=0} = \mu I(t)$$

where U is the internal energy of the electron-lattice system, μ is the absorption coefficient and varies dynamically as the process gives rise to increase in T_e which in turn increases the free electron concentration, on which μ depends. The absorption coefficient μ is modeled following the work of Lin and Cheng (1981). We have not considered here the detailed quantum mechanical processes involved in the absorption of laser power by the semi-conducting material (James, 1983) except those described by Eq. 9, 11 and 12, for we are interested in the computation of $\langle T_e(t)\rangle$ for different thickness, d of the semi-conducting thin film and laser power intensity for 1 ns pulse. The detailed processes of laser power by semi-conducting material is described by Fujimoto *et al.* (1984).

The other boundary condition that exist at the surface is

$$-K_t \frac{\partial T_e}{\partial z} = I_0(1-R)\exp\left(-\left\{\frac{t-\tau}{2\tau}\right\}^2\right) \quad (11a)$$

for Gaussian pulse

$$-K_t \frac{\partial T_e}{dz} = I_0 \text{ for } 0 \le t \le \tau \quad (11b)$$

$$-K_t \frac{\partial T_e}{dz} = 0 \text{ with square pulse for } t > \tau. \quad (12)$$

Both T_e and T_l in Eq. 3-12 are functions of t and z. The other boundary condition assumed in the simulation is:-

$$T_e(t = 0, z) = T_l(t = 0, z) = 300 \text{ k for all z.}$$

The quantity that is of interest to us is $\langle T_e(t)\rangle$ defined below.

$$\langle T_e(t)\rangle = \frac{1}{N}\sum_{j=0}^{N} T_e(i,j) \text{ where } N\Delta z = d$$
$$= \frac{1}{d}\int T_e(z,t)dz. \quad (13)$$

Assuming the thin semi-conducting film to be uniform as mentioned, $\langle T_e(t)\rangle$ is the temperature that would be expected if all the electrons at different z with temperature $\langle T_e(z, t)\rangle$ were to thermalize at time t.

Analytical solution of (7) and (8) along with the above boundary conditions and expressions for C_e and α is nearly impossible. One needs to resort to numerical analysis for a given I_0, τ and d. We took N = 2000. This means a given thickness d of thin film is divided into 2000 equal parts. We also subdivided the pulse with τ = 1 ns in 1000 parts i.e., i = 1 to 2000 and calculate $T_e(i,j)$and $T_l(i,j)$ and obtained $\langle T_e(i)\rangle$ and $\langle T_l(i)\rangle$ for different values of I_0 considering intrinsic GaAs thin films of different thickness.

For metallic tungsten W($5d^4 6s^2$) we can take $C_e = \gamma T_e$ for $T_e < T_F$ which is reasonably satisfied even for T_e approximately equal to 4000 K, since for W

$$T_F = \frac{\hbar^2}{2m_e K_B}\left(3\pi^2 n_e\right)^{\frac{3}{2}} \rightarrow \text{is} \sim 11\times 10^4 \text{K},$$
$$\gamma = \frac{\pi^2 n e K_B^2}{2E_f} \quad (14)$$

Here in tungsten unlike semi-conducting film n_e is a constant and hence γ can be assumed to be constant during the free electron laser heating.

We have carried out the simulation of electron-lattice temperature in thin films of tungsten for femtosecond laser irradiated tungsten (Fig. 2), (which had earlier been studied by other workers) to cross-check our methods of calculation for semi-conducting thin film. We found our method of calculation for tungsten to be in line with the simulations of Bloembergen *et al.* (1975) before applying it to semiconductors thin film. For tungsten thin films

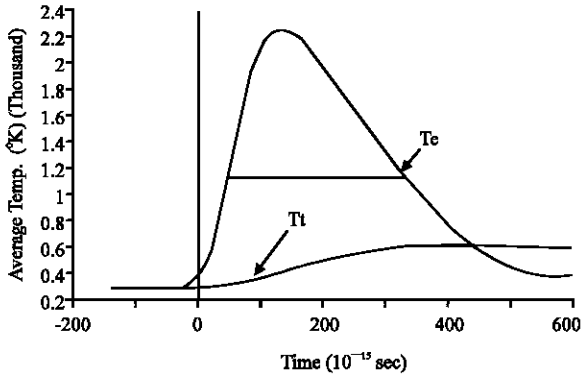

Fig. 2: T_e = Electron temperature of Tungsten T_l = Lattice temperature of Tungsten, Transient Electron Temperature in tungsten irradiated with 75 fs Laser pulse of 16 GW cm^{-2} on a film of thickness 400 A°. τ = 75 fs

electron concentration in conduction band remains practically constant during the laser heating (barring those that may be emitted by thermionic emission).

CALCULATION OF PUMPED FREE ELECTRON CONCENTRATION

As the incident CO_2 laser power is absorbed by the semi-conducting thin film surface the electron temperature rises in comparison with the lattice temperature. The electron stays hot with respect to the lattice for a time much greater than the width of the laser pulse as shown in Fig. 2-5.

Figure 2 shows the result of simulation for 400A^0 thin film of tungsten with 16 GW cm^{-2} laser pulse of 75 fs (10^{-15}s) duration. We clearly see that the electronic temperature T_e rises much faster than the corresponding lattice temperature and there is clear non- equilibrium between T_e and T_l.. The FWHM (full width at half maximum) of the maximum temperature is about 300 fs. The electrons stay at a temperature of 1100 ^{0}K and in non-equilibrium with the lattice. Here we assumed a electron-phonon coupling of 10^{17}. This result is similar to that of Bloembergen *et al.* (1984) and supports the numerical method applied for the solution of T_e, T_l from above in Eq. (4-11), for GaAs thin film.

Figure 3a shows the results of simulation for 280 A^0 thick tungsten and GaAs thin films using 10 MW cm^{-2} peak power laser pulse of 1 ns duration. It is seen that in the case of metal W, both T_e and T_l are at the same temperature, while T_e^s and T_l^s are significantly different. For metal the equilibrium between T_e and T_l in nanosecond pulse regime is well known. The non-

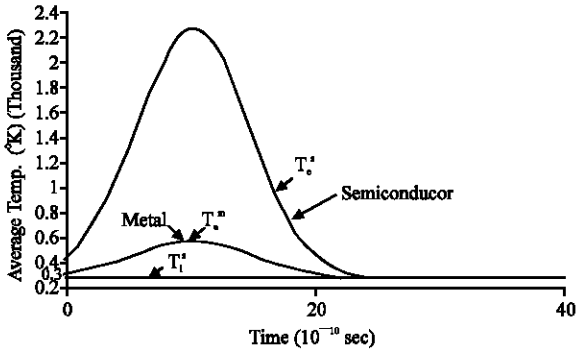

Fig. 3a: Transient electron temperature profile in GaAs with t = 1ns the thickness. The film thickness = 2.8 × 10-6 cm = 280 A^0. It is seen that due to low electron phonon coupling in semi conductor, the electron temperature is much higher than the corresponding lattice temperature T_l. The lattice temperature for metal W is the same as that of electron temperature. A_0 = 10 MW/cm^2, d = 280 A^0

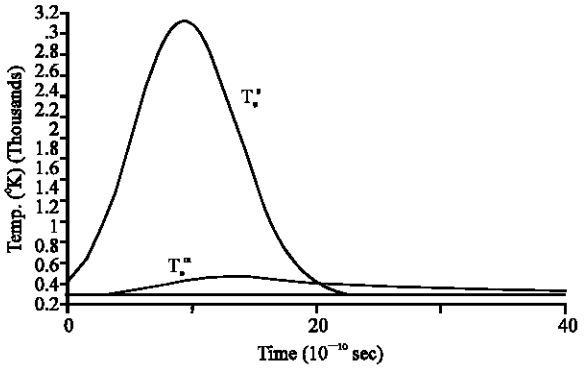

Fig. 3b: The graph for thin film electron and lattice temperature (thousands of Kelvin). Laser Peak Intensity A_0 = 5 MW/cm^2, t = ins. D = 100 A^0. Transient Electron Temperature Profile in a thin film of GaAs with nanosecond laser irradiation. Pulse Width = 1 ns

equilibrium between T_e and T_l in case of semiconductors even in nanosecond pulse regime is new and not investigated before.

Figure 3b shows results of simulation for 5 MW cm^{-2} peak power pulse (τ = 1 ns) using 100A^0 thin film of GaAs and W. In the case of W, the T_e and T_l are inseparable in nanosecond whereas for GaAs a distinct non-equilibrium between T_e and T_l exist over a period greater than the pulse duration of the laser.

Figure 4 shows the simulation of $\langle T_e(t) \rangle$ for GaAs thin films of thickness 0.9, 1.1 and 1.2 μm (1 μm = 10^{-6}

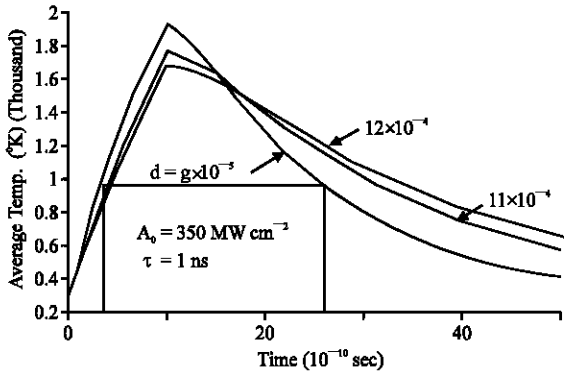

Fig. 4: Different thickness of thin film. Transient electron temperature Profile for different thickness ($d_1 = 9\times10^{-5}$m $d_2 = 1.2\times10^{-4}$ m, $d_3 = 1.1 \times10^{-4}$ m) of thin film for the square pulse

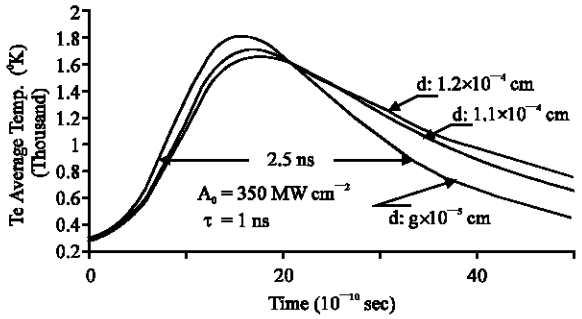

Fig. 5: Different thickness of thin film. Transient electron temperature profile for different thickness ($d_1 = 9\times10^{-5}$m $d_2 = 1.2\times10^{-4}$ m, $d_3 = 1.1 \times10^{-4}$ m) of thin film for the gaussian pulse

m =10^{-4} m) for a square pulse, for a given peak-power of the incident laser intensity. The simulation shows that $\langle T_e(t)\rangle_{max.}$ depends on thickness of the film when the peak power and duration are held constant. It also shows that the decay to equilibrium temperature depends on the $\langle T_e(t)\rangle_{max.}$ lower $\langle T_e(t)\rangle_{max.}$ correspond to lower excitation. For higher $\langle T_e(t)\rangle_{max.}$ the decay is expected to be faster because of faster transfer of energy to lattice as a result of increased electron-phonon coupling. This calculation seems to be in agreement with that of Jensen *et al.* (2003).

Figure 5 shows the simulation of $\langle T_e(t)\rangle$ for GaAs thin films of thickness 0.9, 1.1 and 1.2 μm for a Gaussian pulse peak-power of 350 MW $^{-}$cm^2 of the incident laser intensity. Like Fig. 4, it also shows that $\langle T_e(t)\rangle_{max.}$ depends on the thickness of the film when the peak power and duration are both held constant. The decay is slower than square pulse and lasts longer for longer film thickness.

As discussed earlier, in our simulation for GaAs film, α changes dynamically. Thus the decay rate also changes dynamically as reflected in the three curves in Fig. 4 and 5 depending on the film thickness.

Our investigations shows that the FWHM of the T_e-t profile depends on many parameters like, the semi-conducting material, thickness of the thin film, the width of the laser pulse and its intensity etc. The $T_e(t)$ profile would change with doping concentration in n-type GaAs. For enhanced photoemission from such laser pumped free-electron concentration in thin film semiconductors, what is important is the FWHM and $T_e$max/2 that will determine the enhanced free electron concentration of $n_e(T_e)$ in the conduction band of the semiconductor. To calculate the new n_e as a function of T_e, we can follow two procedures:-

- We assume that the relation (2) still holds at increased T_e then use to compute $n_e(T_e)$. The $n_e(t)$ can then be obtained using the computed relation of $T_e = T_e(t)$ for a given thickness of thin film and incident laser intensity.
  Computed values of $n_e(t)$ are shown in Plots 6-9.
- Following James one can calculate the exponential growth rate η as a function of T_e and then based on calculations presented here one can obtain $T_e(t)$ profile which then give us the η as a function of time for the CO_2 laser pulse irradiation with a given intensity and duration of a semi-conducting thin film of given thickness. Then the new n_e can be computed using the following relation.

$$n_e = n_{e0} \exp \int_0^t \eta(t)\,dt \qquad (15)$$

Our detailed calculation of n_e using above method will be presented on special request.

Transient electron temperature profile enhanced free electron concentration in intrinsic GaAs with 3.5×10^8 W/cm^2 and pulse width $\tau = 10^{-9}$ seconds. Due to two electron-phonon coupling in semiconductors T_e is much higher, T_l for metals is the same as that of T_e. d = 280A^0 We now applied the expression for our simulation as and using (2) for concentration in semiconductor to calculate the concentrations at $\langle T_e(i)\rangle$ and $\langle T_l(i)\rangle$ at time t. Here E_g is the energy gap, M_e^*, M_h^* are the effective mass of the electron and hole respectively. We used $M_e^* = M_h^* = 0.07\ M_e$ (Lin and Cheng, 1981) and E_g = 1.43 eV. The graphs concentrations verses time profile is plotted as shown in Plots 6-9. for various intensities and thickness.

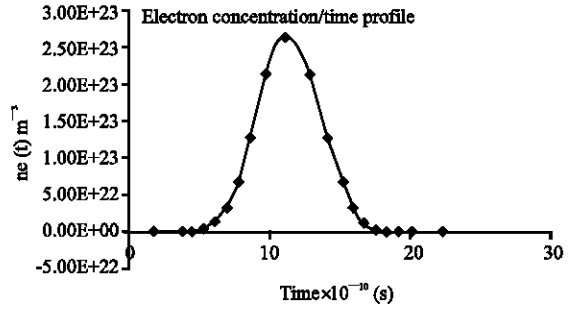

Fig. 6: Transient electron concentration profile in GaAs With 10 MW cm^{-2} and pulse width τ, = 1ns. Thin film thickness = 280 A^0

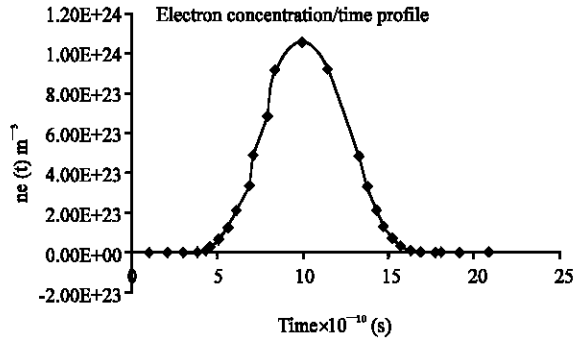

Fig. 7: Transient electron concentration profile in GaAs With 5 MW cm^{-2} and pulse width τ, = 1ns. Thin film thickness = 100 A^0

Figure 6 shows the result of simulations for 280 A^0 of GaAs thin films using a moderate power intensity of 10 MW cm^{-2} peak power laser pulse of 1 ns duration.

Figure 7 shows the result of simulations for 100 A^0 of GaAs thin films using a moderate power intensity of 5 MW cm^{-2} peak power laser pulse of 1 ns duration.

Figure 8 shows the result of simulations for 280 A^0 of GaAs thin films using a moderate power intensity of 3.5x 10^8 W cm^{-2} peak power laser pulse of 1 ns duration for a square pulse.

Figure 9 shows the result of simulations for different thicknesses of GaAs thin films using a moderate power intensity of 3.5× 10^8 W cm^{-2} peak power laser pulse of 1 ns duration for a Gaussian pulse.

It is seen from Fig. 6-9 that the concentration increases dynamically as the time increases as well as the electron temperature and the decreases. This is expected as electrons are first heated and the energy gradually transferred to the lattice in which the whole system thermalized and the source is switched off by the pumped probe laser technique. Then the concentration of the charge carrier decay gradually as shown by the curves (2-5), respectively.

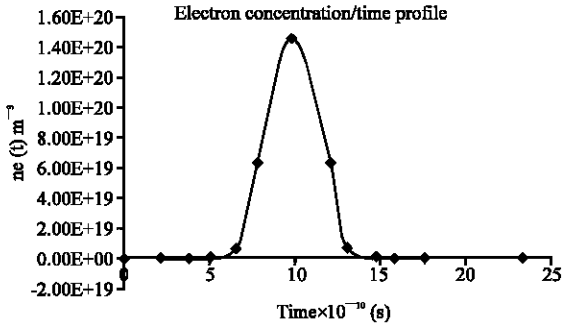

Fig. 8: Transient electron concentration profile in GaAs. With 350 MW cm^{-2} and pulse width τ, = 1 ns. Thin film of different thicknesses d = 1.2×10^{-6} m, 1.1×10^{-6} m, 9×10^{-7} m

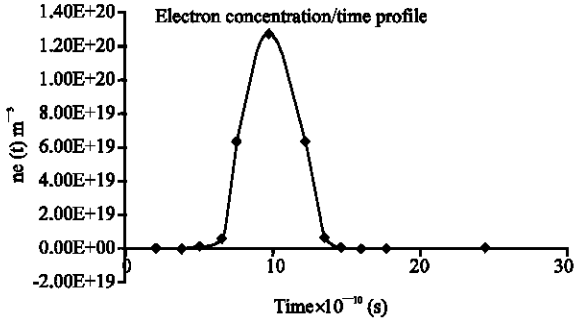

Fig. 9: Transient electron concentration profile in Ge. With 350 MW cm^{-2} and pulse width τ, = 1ns. Thin film of different thicknesses d = 1.2×10^{-6} m, 1.1×10^{-6} m, 9×10^{-7} m

Thus theoretical investigation shows that semi-conducting film offers an ideal medium of observing non-equilibrium between electron and lattice temperatures in the nanosecond laser pulse regime. For practical application of these findings, what is important is that one needs to have thin film of proper thickness matching the peak power available laser pulse intensity such that T_e stays sufficiently hot (say above 1000 K) over a period three to four times the width of the pump laser pulse, so that a suitably delayed probe laser will be able to photo-emit the hot electrons out of the surface (held at high negative potential with the respect to accelerating anode).

PROPOSED EXPERIMENTAL SET UP

The experimental set-up of the electron source of the photocathode is shown diagrammatically in Fig.10 and 11. The photocathode consist of a vacuum tube prepared using an oxide-free technique in a glove box environment. The semiconductor thin films are chemically cleaned and

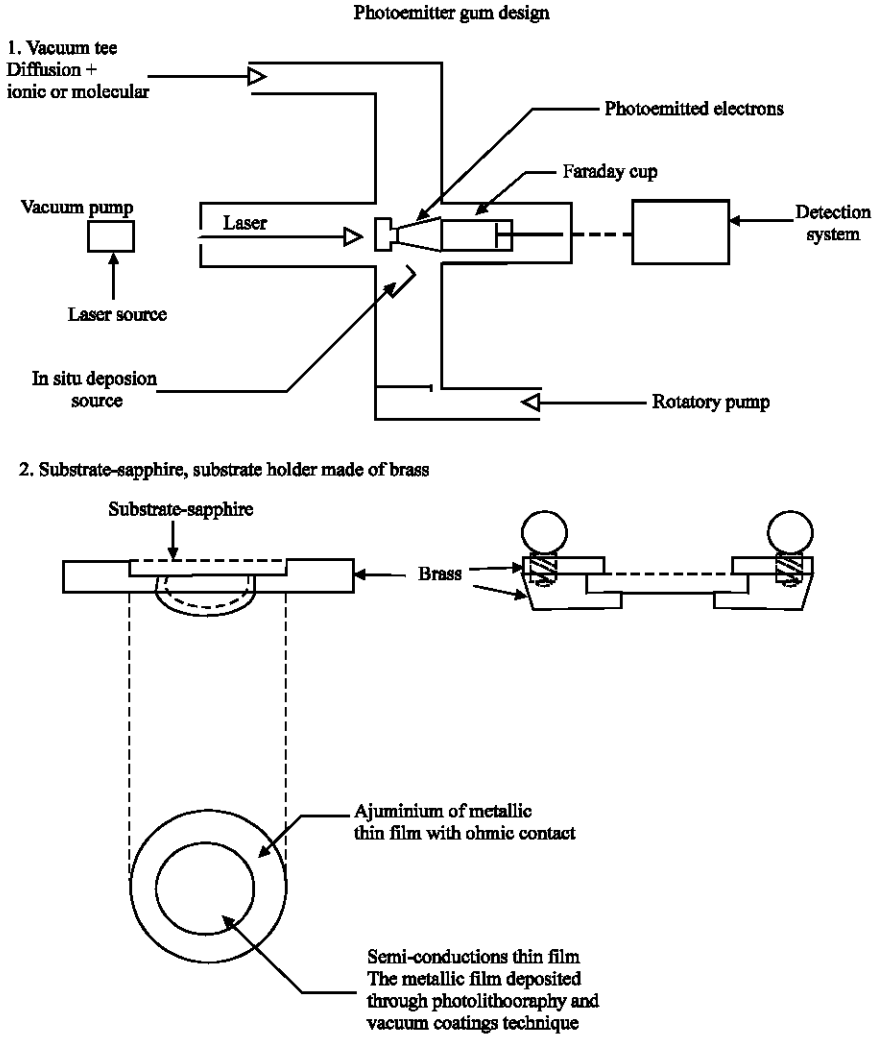

Fig. 10: Diagrammatical representation of photoemtter

transported in a transfer vessel to the load-lock chamber. From there, they are transferred to the preparation chamber. After the growth they are transferred to the photo emitter gun assembly design shown below. Negative electron affinity is obtained after deposition of cesium and oxygen on the photocathode surface which is deposited in in-situ condition by low thermal evaporation in high vacuum condition (10^{-11} to 10^{-12} torr or, mm of Hg). Such high vacuum is achieved through successive use of rotatory pump, diffusion pump, ion or molecular pump along with liquid nitrogen trap. The detail of the arrangement of the vacuum pump is however not shown in the Photo-Emitter Gun assembly (PEG) design (Fig. 10 and 11).

In the PEG design, we proposed that the semi-conducting material be grown on a sapphire substrate which is transparent and can be irradiated by laser pulse from the back, if needed. In the proposed photo-emitter design, the thickness of the semi-conducting film is only of the order of a micron. If the pump and probe laser are to irradiate the semiconductor/metallic film from the front, then much thicker film can be used. As shown earlier by the theoretical calculations, the hot electron temperature and time-profile depend on incident laser power apart from the semi conducting/metallic properties and thickness.

For the laser irradiation the laser pulse from an external source has to pass through a vacuum widow which is to be placed on the laser entrance at the tail of the laser arrow in Fig. 10. The vacuum window can be made of two quartz foils of a few microns thick. Two foil windows prevent catastrophic implosion, if by chance any one of them develops any pinholes during construction. MYLAR foils (Ziegler *et al*., 1996) can also be attempted.

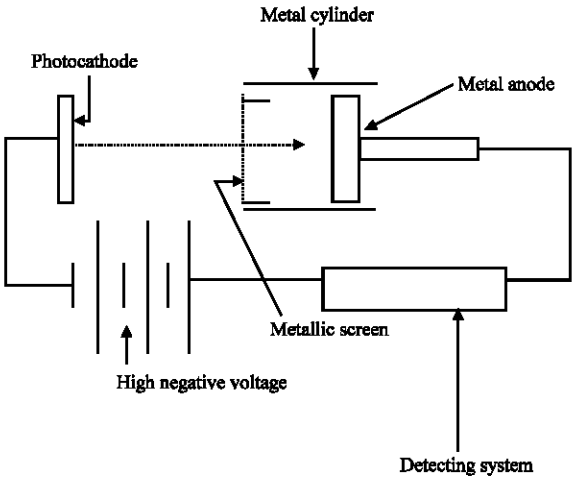

Fig. 11: Diagrammatical representation of faraday cup

The main vacuum chamber of the tube should be operated at a pressure of 10^{-9} mbar. Since the photoemission gun is run in the 10^{-12} mbar regimes, a differential pumping stage using a small diaphragm should be mounted at the exit of the electron gun chamber to sustain the vacuum pressure difference. The pulsed laser beam is focused onto the surface of the photocathode and the extracted pulsed electron beam will be transported to the center of the Faraday cup by means of a superimposed longitudinal magnetic guiding field assists to focus the beam to a desired diameter of below 100 μm at the target (not shown in Fig. 10). Instead of magnetic field guiding electrostatic field guiding can also be used by suitable design of the cathode (containing the photo emitter) and the anode. The pump and probe laser arrangement and the electronic delay between them is not shown in the set-up.

CONCLUSION

Our theoretical investigation shows that with nanosecond CO_2 laser pump irradiation of semi-conducting thin film surfaces, it is possible to create significant non-equilibrium between electron-lattice temperatures. The average electron temperature $\langle T_e(t)\rangle_{max.}$, the FWHM of the $T_e(t)$ verses time profile, depend on laser power intensity, thin film thickness, the incident laser intensity time profile and duration τ and property of the semiconductor materials. Increased T_e corresponds to increased free electron (in conduction band) concentration n_e along with corresponding increase in hole concentration. By suitably adjusting the above parameter (so that the damage threshold for nanosecond pulse is not reached), it is possible to increase n_e in semi-conducting materials significantly for a time scale of the order of 1 nanosecond. Two types of photo emitted electron-beam could be expected from such laser pumped electrons. The first is RLD types (Tensen *et al*., 2003) and the other using a probe laser with probe width of 1 nanosecond (and within the FWHM period of the T_e profile) of suitable frequency (hv probe > Φ. It is expected that the pump probe technique should give rise to enhanced photo emitted electron-beam of charge content greater than so far obtained from femto, picosecond laser irradiated metallic cathodes. Apart from the enhanced photoemission, the above pump technique could also be used for studies of nanosecond electron-dynamics of semi-conducting surfaces.

Thermionic sources if used for FELs cannot be switched on the picosecond time scale and the resultant emittance of the electron beam is too large to allow for Lasing (FEL) at desired wavelength. Instead of computing the actual transient dynamical processes involved in laser-heating of electron gas in dispenser metal cathode, Jensen *et al*. (2003) assumed adhoc electron temperature variation with z through the equation.

$$T_e(z) = T_0 + \left[T_e(0) - T_0 \exp\left(\frac{-z}{1}\right)\right] \qquad (16)$$

Unlike that of Jensen *et al*. (2003) where the electron-temperature (is in equilibrium with metal lattice) is forced to have the same time profile as the laser pulse, our detailed theoretical analysis and the numerical analysis show that the time-profile of electron T_e depends on laser power intensity, the thickness of the semi-conducting thin film and characteristics of the semi-conducting materials and the time profile shape of the laser pulse. The enhanced free electron-gas remains hot over a time longer than the duration of the laser pulse. It may be mentioned that thin film semi-conductors offer a wide range of materials to verify experimentally our above theoretical results. The applications to the creation of high-brightness and low emittance FEL may then be obvious.

REFERENCES

Anisimov, S.I., B.L. Kapeliovich and T.L. Perel`man, 1974. SOV. Phys. JEPT., 39: 375.

Bechtel, J.H., W.L. Smith and N. Bloembergen, 1975. Opt. Commun., 13: 56.

Damascelli, A., G. Gabetta, A. Lumachi, L. Fini, F. Parmigiani, 1996. Phys. Rev., B54: 6031-6034.

Elsayed-Ali, H.E., T. Juhasz, G.O. Smith and W.E. Bron, 1991. Phys. Rev., B43: 4488.

Elseyed-Ali, H.E., T.B. Novris, M.A. Pessot and G.A. Maurou, 1987. Phys. Rev. Let., 58: 1212.

Fann, W.S., R. Storz, H.W.K. Tom and Bokor, 1992. Phys. Rev. Let., 68: 2834.

Fujimoto, J.G., J.M. Liu, E.P. Ippen and N. Bloembergen, 1984. Phys. Rev. Let., 53: 1837-1840.

Grove, A.S., 1967. Physics of Semiconductor Technology (John Wiley and Sons, California, 1967), pp: 102-103.

Hertel, T., E. Knoesel, M. Wolf and G. Ertl, 1996. Phys. Rev. Let., 76: 535.

James, R.B., 1983. J. Applied Phys., 54: 3220- 3224.

Jensen, K.L., D.W. Feldman, M. Virgo and P.G. O`shea, 2003. Phys. Rev. Special Topics, 6: 083501-083514.

Kaganov, M.I., I.M. Lifshitz and L.V. Tanatarov, 1956. SOV. Phys. JETP., 4: 174.

Lin, S.W. and Y. Cheng, 1981. Chinese J. Phys., 19: 76-86.

Scheonlein, R.W., J.G. Fujimoto, G.L. Eesley and T.W. Capehart, 1988. Phys. Rev. Let., 61: 2596.

Stephen Benson, V., 2003. Optics and Photonics News, pp: 21-25.

Sun, C.K., F. Valle'e, L.H. Acioli, E.P. Ippen and J.G. Fujimoto, 1994. Phys. Rev., B50: 15337.

Wang, X.J., 2002. Progress and future Direction in Brightness Electron Beam sources. Proceeding New York 11973 USA. Supported by USDOE contract. DE-AC02-98CH10886, pp: 2.

Wang, X.Y., D.M. Riffe, Y.S. Lee and M.C. Downer, 1994. Phys. Rev., B50: 8016.

Wu, J.L., Q.F. Zhang, C.M. Wang and Y.H. Zou, 2001. Applied Sur. Sci., 183: 80-85.

Yen, R., J. Liu and N. Bloembergen, 1980. Opt. Commun., 35: 277.

Ziegler, J.F., P.A. Saunders and T.H. Zabel, 1996. Portable faraday cup for nonvacuum proton beams. IBM Resource Dev., 40: 73-75.